電弱バリオン数生成の現状と課題

瀬名波 栄問

October 18, 2013

Abstract

Electroweak baryogenesis is reviewd in light of the 126 GeV Higgs boson. In this talk, we focus on the minimal supersymmetric standard model (MSSM) and investigate an overlooked issue associated with a high-temperature expansion of the two-loop effective potential. As a first step toward the complete analysis of the MSSM, we consider the $U(1)$ gauge theory and devise a tractable calculation scheme that can greatly simplify the sunset diagrams involving the gauge bosons without using the high-temperature approximation.

1 Introduction

According to the cosmological data, the baryon asymmetry of the universe (BAU) is found to be $\eta = n_b/n_\gamma \simeq 10^{-10}$ [1]. Clarification of the origin of the BAU is one of the greatest challenges in particle physics, cosmology and nuclear physics. If the BAU is generated before $T = \mathcal{O}(1)$ MeV, the light element abundances (D,^{3}He,^{4}He,^{7}Li) can be explained by the standard Big-Bang cosmology. To get the right η (which is called baryogenesis) from an initially baryon symmetric Universe, the so-called Sakharov's conditions have to be satisfied [2]: (i) baryon number (B) violation, (ii) C and CP violation, (iii) departure from thermal equilibrium. To this end, a lot of scenarios have been proposed so far [3]. From an experimental point of view, electroweak baryogenesis (EWBG) [4] among others is the most testable scenario, and thus it is in urgent need of detailed analysis in the LHC and future ILC eras.

It is known that the possibility of the EWBG in the standard model (SM) has been ruled out due to the lack of sufficiently large CP violating effect and absence of the strong first-order phase transition (EWPT) which is needed for satisfying the Sakharov's condition (iii). Such a shortcoming of the SM motivates us to look for physics beyond the SM. Much attention has been paid to the minimal supersymmetric standard model (MSSM) as a leading candidate for new physics.

In this talk, after reviewing the EWBG mechanism briefly, we derive the sphaleron decoupling condition in light of the 126 GeV Higgs boson. In order to know a prescription for the baryogenesis problems in the SM, the EWPT is also reviewed using the one-loop effective potential. Then, we move on to the MSSM and point out the unresolved issues shortly. After presenting our new calculation method that can solve one of the issues, we apply it to the $U(1)$ gauge theory as a first step toward the complete analysis of the MSSM EWBG.

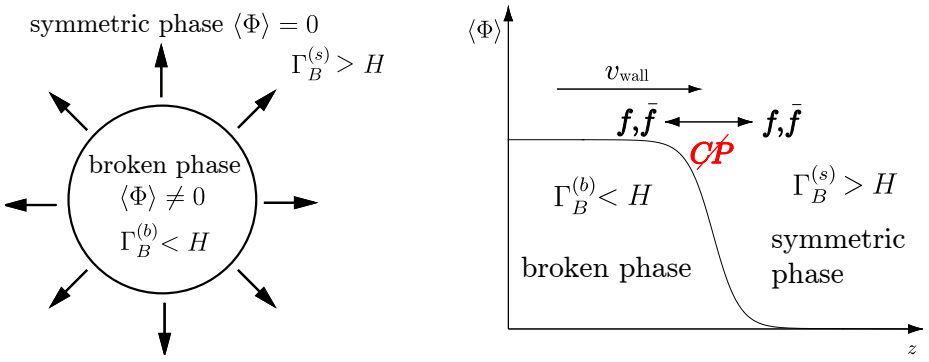

Figure 1: (Left) The bubble expansion. (Right) The Higgs VEV as function of z which is the direction of the bubble expansion.

2 EWBG mechanism

Foregoing Sakharov's conditions in the EWBG are satisfied as follows: (i) B violation is realized by an anomalous process at finite temperature (conventionally referred as *sphaleron process* although the sphaleron solution does not exist in the symmetric phase.) (ii) C is maximally violated by the chiral gauge interactions, CP violation comes from the Cabbibo-Kobayashi-Maskawa matrix or other complex parameters once the standard model (SM) is extended. (iii) Out of equilibrium is realized by the first-order EWPT with bubble nucleation and expansion.

The left panel of Fig. 1 shows a schematic picture of the expanding bubble wall. The inside of the bubble corresponds to the broken phase where the Higgs vacuum expectation value (VEV) is nonzero, $\langle\Phi\rangle \neq 0$ while the outside of it represents the symmetric phase where $\langle\Phi\rangle = 0$. In the right panel of Fig. 1, $\langle\Phi\rangle$ is depicted as a function of z which is a direction of the bubble expansion. The outline of the EWBG is as follows.

1. Because of CP violation induced by interactions between the bubble and the particles in the plasma, chiral charges are asymmetrized.
2. They diffuse into the symmetric phase and accumulate.
3. B is generated via sphaleron process.
4. After decoupling of the sphaleron process in the broken phase, B is fixed.

The last step may leave a detectable footprint in low energy observables. In the following, we will look into one of such possibilities.

3 Sphaleron decoupling condition

In order to preserve the generated BAU via the sphaleron process in the symmetric phase, the B-changing rate in the broken phase ($\Gamma_B^{(b)}$) must be sufficiently suppressed. Namely,

$$\Gamma_B^{(b)}(T) \simeq (\text{prefactor}) e^{-E_{\rm sph}(T)/T} < H(T) \simeq 1.66\sqrt{g_*(T)}T^2/m_{\rm P} \tag{3.1}$$

is satisfied, where $E_{\rm sph}$ denotes the sphaleron energy, g_* is the degrees of freedom of relativistic particles in the plasma ($g_* = 106.75$ in the SM) and $m_{\rm P}$ stands for the Planck mass which is about 1.22×10^{19} GeV. Since $E_{\rm sph}$ is proportional to the Higgs

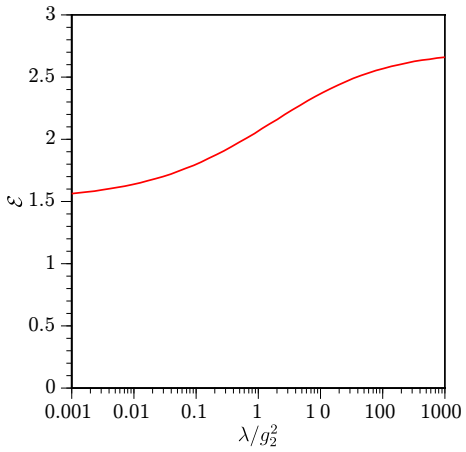

Figure 2: The dimensionless sphaleron energy $\mathcal{E}(0)$ vs. λ/g_2^2.

VEV (denoted by v), Eq. (3.1) can be realized if the EWPT is strongly first-order. Conventionally, the sphaleron energy is parametrized as $E_{\rm sph}(T) = 4\pi v(T)\mathcal{E}(T)/g_2$, where g_2 denotes the SU(2) gauge coupling constant. Eq. (3.1) is then cast into the form

$$\frac{v(T)}{T} > \frac{g_2}{4\pi\mathcal{E}(T)}\Big[42.97 + \text{log corrections}\Big]. \tag{3.2}$$

The dominant contributions on the right-hand side is $\mathcal{E}(T)$ while the log corrections that mostly come from the zero mode factors of the fluctuations about the sphaleron typically amount to about 10% [5].

As an illustration, we evaluate the sphaleron energy at zero temperature, $\mathcal{E}(0)$, within the SM [6]. Since the $\mathrm{U}(1)_Y$ contribution is sufficiently small [7], it is enough to confine ourself to the $\mathrm{SU}(2)_L$ gauge-Higgs system. To find the sphaleron solution, we adopt a spherically symmetric configurations ansatz with a noncontractible loop [6].

In Fig. 2, $\mathcal{E}(0)$ is plotted as a function of λ/g_2^2. We can see that as λ/g_2^2 increases, $\mathcal{E}$ increases. For the Higgs boson with a mass of 126 GeV, which corresponds to $\lambda \simeq 0.13$, one finds $\mathcal{E}(0) \simeq 1.92$. With this value, Eq. (3.2) becomes

$$\frac{v(T)}{T} > 1.16, \tag{3.3}$$

where only the dominant contributions are retained on the right-hand side in Eq. (3.2). Note that the use of $\mathcal{E}(0)$ in the decoupling criterion leads to somewhat underestimated results since $\mathcal{E}(T) < \mathcal{E}(0)$. In the MSSM, using the finite-temperature effective potential at the one-loop level, $v(T_N)/T_N > 1.38$ is obtained, where the sphaleron energy as well as the translational and rotational zero mode factors of the fluctuation around the sphaleron are evaluated at a nucleation temperature (T_N) which is somewhat below T_C [5].

4 Electroweak phase transition

Here, we explicitly demonstrate why the SM EWBG fails, which may give a signpost searching for new physics. Using a high-temperature expansion, the one-loop effective

potential at finite temperature is reduced to

$$V_{\rm eff}(\varphi;T) \simeq D(T^2-T_0^2)\varphi^2 - ET\varphi^3 + \frac{\lambda_T}{4}\varphi^4, \tag{4.1}$$

where

$$D = \frac{1}{8v^2}\Big(2m_W^2+m_Z^2+2m_t^2\Big), \quad E = \frac{1}{4\pi v^3}\Big(2m_W^3+m_Z^3\Big) \simeq 10^{-2}, \tag{4.2}$$

$$\lambda_T = \frac{m_h^2}{2v^2}\left[1-\frac{3}{8\pi^2v^2m_h^2}\left\{2m_W^4\log\frac{m_W^2}{\alpha_B T^2}+m_Z^4\log\frac{m_Z^2}{\alpha_B T^2}-4m_t^4\log\frac{m_t^2}{\alpha_F T^2}\right\}\right], \tag{4.3}$$

with $\log\alpha_B = 2\log 4\pi - 2\gamma_E \simeq 3.91$ and $\log\alpha_F = 2\log\pi - 2\gamma_E \simeq 1.14$. Appearance of the cubic term with the negative coefficient dictates that the EWPT should be first-order. Note that since the origin of the cubic term is the zero Matsubara frequency mode, the only bosonic thermal loops contribute to E.

The critical temperature T_C is defined by a temperature at which $V_{\rm eff}(\varphi;T)$ has two degenerate minima. At T_C, $V_{\rm eff}$ takes the form

$$V_{\rm eff}(\varphi;T_C) = \frac{\lambda_{T_C}}{4}\varphi^2(\varphi-v_C)^2, \quad v_C = \frac{2ET_C}{\lambda_{T_C}}. \tag{4.4}$$

As we discussed in the previous section, $v_C/T_C \gtrsim 1$ should hold to avoid the washout by the sphaleron in the broken phase. Since $\lambda_{T_C} \simeq m_h^2/2v^2$, one obtains the upper bound of the Higgs boson mass as

$$m_h \lesssim 2v\sqrt{E} \simeq 48 \text{ GeV}. \tag{4.5}$$

This mass range has been already excluded by the LEP experiments. According to nonperturbative studies, the EWPT in the SM is a crossover for $m_h \gtrsim 73$ GeV [8].

From the above argument, one of the straightforward way-outs is to enhance E by adding the bosonic degrees of freedom.

5 Light stop scenario in the MSSM

Let us consider the MSSM case. The EWBG scenario in this model is the so-called "light stop scenario (LSS) [9]", which is now on the verge of being excluded. (see e.g. [10, 11]).

In order to realize the physical Higgs boson mass, the left-handed stop SUSY breaking mass ($m_{\tilde{q}}$) has to be much greater than the right-handed one ($m_{\tilde{t}_R}$). According to [11], $m_{\tilde{q}}$ may be as large as $\mathcal{O}(10^6)$ TeV. In such a case, the effective theory approach is more appropriate. The effective theory of the LSS is constructed in [12] and is applied to the EWBG [13, 11]. Here, to make our analysis simple, we take m_h as an input.

In the limit of $m_{\tilde{q}} \gg m_{\tilde{t}_R}$, the stop masses are reduced to

$$\bar{m}_{\tilde{t}_2}^2 = m_{\tilde{q}}^2 + \frac{y_t^2\sin^2\beta}{2}\left(1+\frac{|X_t|^2}{m_{\tilde{q}}^2}\right)\varphi^2 + \mathcal{O}(g^2) \simeq m_{\tilde{q}}^2, \tag{5.1}$$

$$\bar{m}_{\tilde{t}_1}^2 = m_{\tilde{t}_R}^2 + \frac{y_t^2\sin^2\beta}{2}\left(1-\frac{|X_t|^2}{m_{\tilde{q}}^2}\right)\varphi^2 + \mathcal{O}(g^2), \tag{5.2}$$

where $X_t = A_t - \mu/\tan\beta$. As discussed above, the heavy stop does not play any role as far as the first-order EWPT is concerned. Also, the small $m_{\tilde{t}_R}^2$ and X_t are desirable. More precisely, at finite temperature, the light stop receives a thermal correction

$(\Delta m^2_{\tilde{t}_R}(T))$ which is of the order of T^2 to leading order. So the $m^2_{\tilde{t}_R} + \Delta m^2_{\tilde{t}_R}(T)$ should be vanishingly small for the strong first-order EWPT, which implies $m^2_{\tilde{t}_R} < 0$ since $\Delta m^2_{\tilde{t}_R}(T) > 0$. In the LSS scenario considered in [13], the color-charge-breaking vacuum is the global minimum. On the other hand, the electroweak vacuum is metastable whose lifetime is longer than the age of the Universe.

For simplicity, we take $m^2_{\tilde{t}_R} = 0$ in the following discussion. The coefficient of cubic term in the one-loop effective potential at finite temperature is

$$V_{\rm eff} \ni -(E_{\rm SM} + E_{\tilde{t}_1})T\varphi^3, \quad E_{\tilde{t}_1} = \frac{y_t^3 \sin^3\beta}{4\sqrt{2}} \left(1 - \frac{|X_t|^2}{m^2_{\tilde{q}}}\right)^{3/2}. \tag{5.3}$$

Therefore, $E_{\tilde{t}_1}$ can strengthen v_C/T_C.

5.1 Overlooked issues

There are two problems which have not been properly addressed in the literature, i.e.,
(i) validity of the high-temperature expansion (HTE) of the sunset diagram,
(ii) sphaleron decoupling condition at the two-loop level.
In what follows, we will work out the former issue.

6 Two-loop analysis of thermal phase transition

As a first step toward the analysis in the MSSM, we consider the Abelian-Higgs (AH) model for the sake of simplicity. The Lagrangian of the AH is

$$\mathcal{L} = -\frac{1}{4}F_{\mu\nu}F^{\mu\nu} + |D_\mu\Phi|^2 - V_0(|\Phi|^2), \tag{6.1}$$

where $F_{\mu\nu} = \partial_\mu A_\nu - \partial_\nu A_\mu$, $D_\mu\Phi = (\partial_\mu - ieA_\mu)\Phi$ and The scalar potential is given by

$$V_0(|\Phi|^2) = -\nu^2|\Phi|^2 + \frac{\lambda}{4}|\Phi|^4. \tag{6.2}$$

We parametrize the scalar field in terms of the VEV (v) and fluctuation fields

$$\Phi(x) = \frac{1}{\sqrt{2}}\big(v + h(x) + ia(x)\big), \tag{6.3}$$

where $h(x)$ is a physical state and $a(x)$ is a Nambu-Goldstone boson which is eaten by the gauge boson. The field-dependent scalar and gauge boson masses are

$$m_h^2 = -\nu^2 + \frac{3\lambda}{4}v^2, \quad m_a^2 = -\nu^2 + \frac{\lambda}{4}v^2, \quad m_A^2 = e^2v^2, \tag{6.4}$$

where we work in the Landau gauge. In our study, the $\overline{\rm MS}$ scheme is used for renormalization.

We adopt a resummation method in which temperature-dependent mass terms $[\Delta m^2]$ are added and subtracted in the original Lagrangian [14, 15]. The subtracted terms are considered as the counterterms. As is well known, thermal corrections to the longitudinal and transverse parts of the gauge boson self-energy are different. Consequently, the resummed Lagrangian is obtained as follows.

$$\mathcal{L}_B = \mathcal{L}_R + \mathcal{L}_{\rm CT}$$

$$\to \mathcal{L}_R - \Delta m_\Phi^2 \Phi^\dagger\Phi + \frac{1}{2}A^\mu\Big[\Delta m_L^2 L_{\mu\nu}(i\partial) + \Delta m_T^2 T_{\mu\nu}(i\partial)\Big]A^\nu$$
$$+ \mathcal{L}_{\rm CT} + \Delta m_\Phi^2 \Phi^\dagger\Phi - \frac{1}{2}A^\mu\Big[\Delta m_L^2 L_{\mu\nu}(i\partial) + \Delta m_T^2 T_{\mu\nu}(i\partial)\Big]A^\nu, \tag{6.5}$$

where $\mathcal{L}_{B(R)}$ are denoted by the bare (renormalized) Lagrangian and $\mathcal{L}_{\rm CT}$ by the counterterm. Note that Eq. (6.5) has the gauge invariant form.[1] $L_{\mu\nu}(p)$ and $T_{\mu\nu}(p)$ are the projection tensors which are given by

$$T_{00} = T_{0i} = T_{i0} = 0, \quad T_{ij} = g_{ij} - \frac{p_i p_j}{-\boldsymbol{p}^2}, \tag{6.6}$$

$$L_{\mu\nu} = P_{\mu\nu} - T_{\mu\nu}, \quad P_{\mu\nu} = g_{\mu\nu} - \frac{p_\mu p_\nu}{p^2}, \tag{6.7}$$

in the rest frame of the thermal bath. With the resummed Lagrangian (6.5), the scalar and gauge boson propagators take the form

$$\Delta_h(p) = \frac{1}{p^2 - m_h^2(T)}, \quad \Delta_a(p) = \frac{1}{p^2 - m_a^2(T)}, \tag{6.8}$$

$$\boldsymbol{D}_{\mu\nu}(p) = \frac{-1}{p^2 - m_L^2(T)}L_{\mu\nu}(p) + \frac{-1}{p^2 - m_T^2(T)}T_{\mu\nu}(p), \tag{6.9}$$

where $m_{h,a}^2(T) = m_{h,a}^2 + \Delta m_\Phi^2$ and $m_{L,T}^2(T) = m_A^2 + \Delta m_{L,T}^2$. Explicitly, the thermal masses are, respectively, given by

$$\Delta m_\Phi^2 = \frac{T^2}{12}(3e^2 + \lambda), \quad \Delta m_T^2 = 0, \quad \Delta m_L^2 = \frac{e^2}{3}T^2. \tag{6.10}$$

Although Eq. (6.9) can be used as the resummed gauge boson propagator [15], we can devise a more convenient form for two-loop calculations. Using $L_{\mu\nu}(p) + T_{\mu\nu}(p) = P_{\mu\nu}(p)$, $\boldsymbol{D}_{\mu\nu}(p)$ can be rewritten in terms of $P_{\mu\nu}(p)$ and $T_{\mu\nu}(p)$ or $L_{\mu\nu}(p)$. Let $\boldsymbol{D}_{\mu\nu}^{(r=0)}(p)$ be the former case, and $\boldsymbol{D}_{\mu\nu}^{(r=1)}(p)$ the latter one. The most general expression is cast into the form

$$\begin{aligned}\boldsymbol{D}_{\mu\nu}(p) &= (1-r)\boldsymbol{D}_{\mu\nu}^{(r=0)}(p) + r\boldsymbol{D}_{\mu\nu}^{(r=1)}(p) \\ &= \left[\frac{-(1-r)}{p^2 - m_L^2} + \frac{-r}{p^2 - m_T^2}\right]P_{\mu\nu}(p) + \left[\frac{-1}{p^2 - m_T^2} - \frac{-1}{p^2 - m_L^2}\right]\big(T_{\mu\nu}(p) - rP_{\mu\nu}(p)\big),\end{aligned} \tag{6.11}$$

where r denotes an arbitrary real parameter. Note that the noncovariant part yields less ultraviolet divergent loop integrals. It turns out that loop calculations are greatly simplified if r is chosen such that $g^{\mu\nu}\big(T_{\mu\nu}(p) - rP_{\mu\nu}(p)\big) = 0$, which leads to $r = (d-2)/(d-1)$.

After fixing r, let us denote Eq. (6.11) as

$$\boldsymbol{D}_{\mu\nu}(p) = D_{\mu\nu}^{\rm cov}(p) + \delta D_{\mu\nu}(p), \tag{6.12}$$

With this gauge boson propagator, together with Eq. (6.8), we will compute the effective potential.

It turns out that noncovariant parts of the sunset diagrams involving $\delta D_{\mu\nu}$ do not yield any effects on the thermal phase transition to leading order. For details, see [16].

[1] For non-Abelian gauge theories, however, this resummation method would break the gauge invariance. We also note that the thermal masses of h and a would be different if v-dependent corrections were included, rendering the gauge invariance spoiled. In our analysis, we keep the leading order corrections which are $\mathcal{O}(T^2)$, so the $\Delta m_h^2(T) = \Delta m_a^2(T) = \Delta m_\Phi^2$.

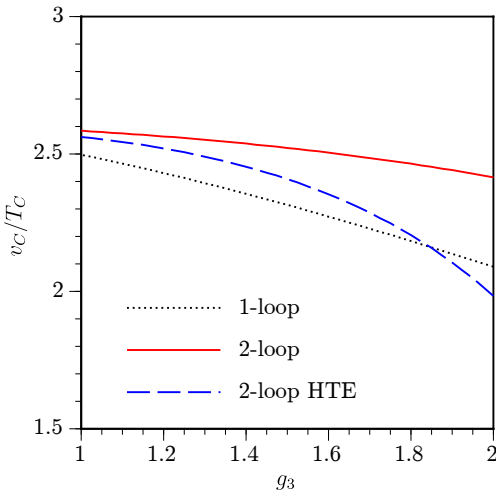

Figure 3: v_C/T_C in the three cases are shown as a function of g_3. The input parameters are given in the text.

6.1 MSSM-like toy model

We discuss the thermal PT using the scheme proposed in the previous section. As a first step toward the complete analysis of the two-loop driven first-order EWPT scenario such as the MSSM, we consider an extended AH model in which additional $U(1)$ gauge boson and complex scalar are introduced. The added Lagrangian is

$$\Delta\mathcal{L} = -\frac{1}{4}G_{\mu\nu}G^{\mu\nu} + |D_\mu\tilde{t}|^2 - (m_0^2 + y^2|\Phi|^2)|\tilde{t}|^2 + \frac{\tilde{\lambda}}{4}|\tilde{t}|^4, \tag{6.13}$$

where $G_{\mu\nu} = \partial_\mu G_\nu - \partial_\nu G_\mu$ and $D_\mu\tilde{t} = (\partial_\mu - ig_3 G_\mu)\tilde{t}$.

In the MSSM the stop-stop-gluon sunset diagram enhances v_C/T_C. We scrutinize this effect with and without the HTE. The explicit forms of the scalar-scalar-vector and scalar-vector-vector type sunset diagrams can be found in Ref. [17]. Those sunset diagrams are composed of $K_{--}(a_1, a_2, a_3)$ and the one-loop finite-temperature functions. Such one-loop thermal functions and two-loop ones of the type of $K(a)$, $K_{--}(a, a, 0)$, $K_{--}(a, 0, 0)$ and $K_{--}(0, 0, a)$ are evaluated by the numerical integrations. For other types of $K_{--}(a_1, a_2, a_3)$ such as $K_{--}(m_h/T, m_a/T, m_a/T)$, the mass-averaging approximation is also employed.

In the following, by the HTE case we mean the following replacements

$$K(a) \to K^{\rm HTE}(a) = -\frac{\pi^2}{3}(\ln a^2 + 3.48871), \tag{6.14}$$

$$K_{--}(a, a, 0) \to K_{--}^{\rm HTE}(a, a, 0) = -\pi^2(\ln a^2 + 3.01398), \tag{6.15}$$

and all the rest are unchanged.

In FIG. 3, v_C/T_C is shown as a function of g_3. We set $v = 246$ GeV, $m_h = 35$ GeV, $m_0^2 = 0$, $y = 1.0$, $e = 0.5$, $\tilde{\lambda} = 0.3$ and $\bar{\mu} = 150$ GeV. Here, we take m_h as an input instead of using λ. This trade is done at a loop level. The red curve represents the two-loop calculation, and the blue dashed curve denotes the two-loop calculation with the HTE. The one-loop calculation of v_C/T_C is also shown by the dotted black curve. This figure shows that enhancement of v_C/T_C due to the $\tilde{t}$-$\tilde{t}$-G_μ diagram can still persist beyond the HTE. In this specific example, the use of the HTE leads to the

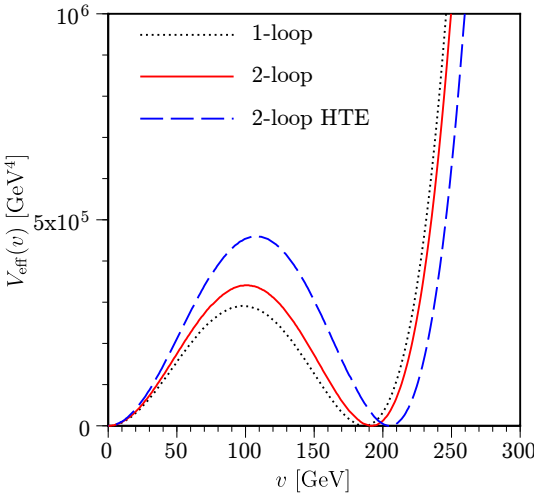

Figure 4: The shown is the effective potential at T_C. We take $g_3 = 1.2$. The remaining parameters are the same as in FIG. 3.

underestimated v_C/T_C. Note that in the limit of $g_3 \to 0$, the results would approach to those in the AH model. In such a limit, the difference between '2-loop' and '2-loop HTE' would be decreasing since the sunset diagrams are less important for the PT analysis. However, we emphasize that evaluation of the sunset diagrams without the HTE is necessary in the MSSM-like model.

The height of the barrier between the two degenerate vacua in the effective potential is also relevant to dynamics of the first-order PT. The effective potentials at T_C and $g_3 = 1.2$ in the three cases are plotted in FIG. 4. The color and line coordinates are the same as in FIG. 3. We find that $v_C/T_C|_{\text{1-loop}} = 186.55/76.75 = 2.43$, $v_C/T_C|_{\text{2-loop}} = 191.84/74.80 = 2.56$ and $v_C/T_C|_{\text{2-loop HTE}} = 204.98/81.31 = 2.52$. The significant increase of T_C in the HTE case may be the consequence of the artificial negative contributions to the quadratic term in the scalar potential. It is also found that the barrier height at the two-loop level is somewhat higher than that of the one-loop case, delaying the onset of the PT. However, we may get the overestimated result once the HTE is used. We observe that generally the larger g_3 can bring the larger errors in v_C, T_C and the barrier height.

7 Summary

In this talk, the current status of electroweak baryogenesis is briefly reviewed. In particular, we focused on validity of the high-temperature expansion of the sunset diagrams in the MSSM. As a first step toward the complete analysis of the MSSM EWBG, we devised a tractable calculation scheme that can be applicable in the $U(1)$ gauge theory. Our results suggest that v_C and T_C can be overestimated if the high-temperature expansion is used. However, the error of v_C/T_C may be within a few percent level. It is concluded that the scalar-scalar-vector type sunset diagram still plays an important role in enhancing v_C/T_C.

References

[1] J. Beringer *et al.* [Particle Data Group Collaboration], Phys. Rev. D **86**, 010001 (2012).

[2] A. D. Sakharov, Pisma Zh. Eksp. Teor. Fiz. **5**, 32 (1967) [JETP Lett. **5**, 24 (1967)] [Sov. Phys. Usp. **34**, 392 (1991)] [Usp. Fiz. Nauk **161**, 61 (1991)].

[3] M. Shaposhnikov, J. Phys. Conf. Ser. **171**, 012005 (2009).

[4] V. A. Kuzmin, V. A. Rubakov and M. E. Shaposhnikov, Phys. Lett. B **155** (1985) 36. For reviews on electroweak baryogenesis, see A. G. Cohen, D. B. Kaplan and A. E. Nelson, Ann. Rev. Nucl. Part. Sci. **43** (1993) 27; M. Quiros, Helv. Phys. Acta **67** (1994) 451; V. A. Rubakov and M. E. Shaposhnikov, Usp. Fiz. Nauk **166** (1996) 493; K. Funakubo, Prog. Theor. Phys. **96** (1996) 475; M. Trodden, Rev. Mod. Phys. **71** (1999) 1463; W. Bernreuther, Lect. Notes Phys. **591** (2002) 237; J. M. Cline, [arXiv:hep-ph/0609145]; D. E. Morrissey and M. J. Ramsey-Musolf, New J. Phys. **14**, 125003 (2012). T. Konstandin, arXiv:1302.6713 [hep-ph].

[5] K. Funakubo and E. Senaha, Phys. Rev. D **79**, 115024 (2009).

[6] N. S. Manton, Phys. Rev. D **28**, 2019 (1983); F. R. Klinkhamer and N. S. Manton, Phys. Rev. D **30**, 2212 (1984).

[7] B. Kleihaus, J. Kunz and Y. Brihaye, Phys. Lett. B **273**, 100 (1991); F. R. Klinkhamer and R. Laterveer, Z. Phys. C **53**, 247 (1992).

[8] K. Kajantie, M. Laine, K. Rummukainen and M. E. Shaposhnikov, Phys. Rev. Lett. **77**, 2887 (1996); K. Rummukainen, M. Tsypin, K. Kajantie, M. Laine and M. E. Shaposhnikov, Nucl. Phys. B **532**, 283 (1998); F. Csikor, Z. Fodor and J. Heitger, Phys. Rev. Lett. **82**, 21 (1999); Y. Aoki, F. Csikor, Z. Fodor and A. Ukawa, Phys. Rev. D **60**, 013001 (1999).

[9] M. S. Carena, M. Quiros and C. E. M. Wagner, Phys. Lett. B **380**, 81 (1996); D. Delepine, J. M. Gerard, R. Gonzalez Felipe and J. Weyers, Phys. Lett. B **386**, 183 (1996).

[10] T. Cohen, D. E. Morrissey and A. Pierce, Phys. Rev. D **86**, 013009 (2012); D. Curtin, P. Jaiswal and P. Meade, JHEP **1208**, 005 (2012); K. Krizka, A. Kumar and D. E. Morrissey, arXiv:1212.4856 [hep-ph].

[11] M. Carena, G. Nardini, M. Quiros and C. E. M. Wagner, JHEP **1302**, 001 (2013).

[12] M. Carena, G. Nardini, M. Quiros and C. E. M. Wagner, JHEP **0810**, 062 (2008).

[13] M. Carena, G. Nardini, M. Quiros and C. E. M. Wagner, Nucl. Phys. B **812**, 243 (2009).

[14] R. R. Parwani, Phys. Rev. D **45**, 4695 (1992) [Erratum-ibid. D **48**, 5965 (1993)].

[15] W. Buchmuller, T. Helbig and D. Walliser, Nucl. Phys. B **407**, 387 (1993).

[16] K. Funakubo and E. Senaha, Phys. Rev. D **87**, no. 5, 054003 (2013) [arXiv:1210.1737 [hep-ph]].

[17] P. B. Arnold and O. Espinosa, Phys. Rev. D **47**, 3546 (1993) [Erratum-ibid. D **50**, 6662 (1994)].